Current Chemistry Letters 11 (2022) 227–236

Contents lists available at GrowingScience

Current Chemistry Letters

homepage: www.GrowingScience.com

An unexpected aerobic oxidation of α-amino boronic acid part of Borteomib, leading to (thermal) decomposition of this very expensive anti-cancer API

Abolghasem Beheshti[a,b], Meghdad Payab[c*], Vahid Seyyed-Ali-Karbasi[a] and Seyyed Amir Siadati[a,d]

[a]*R&D Department, Tofigh Daru Research and Engineering Company, TPICO, Tehran, Iran*
[b]*Department of Chemistry, Payame Noor University, Tehran, Iran*
[c]*Faculty of Chemistry, University of Mazandaran, Mazandaran, Iran*

C H R O N I C L E

Article history:
Received June 29, 2021
Received in revised form
July 20, 2021
Accepted November 18, 2021
Available online
November 18, 2021

Keywords:
Bortezomib
Organic Volatile Impurities (OVI)
Un-expected aerobic oxidation
GC-FID
Stability

A B S T R A C T

This project was started when an unknown peak was being detected in the *organic volatile impurity* (OVI) analysis (using the head-space vapor sampling procedure) of *bortezomib* (BZB) *active pharmaceutical ingredient* (API), in pharmaceutical companies. During the OVI analysis of the API of BZB, a huge-area peak with an unknown source appeared in the chromatograms of the gas chromatography with *flame ionization detector* (GC-FID). The data prepared by GC-MAS revealed that the considered huge peak was 3-methylbutanal (3MBut). But, investigating the synthesis procedures showed that during all the synthesis steps, 3MBut or any other solvent containing this impurity was not being applied. Thus, we had concluded that there is a possibility for emergence of this aldehyde from bortezomib itself. To find out which part of bortezomib might turn into 3MBut, we began to investigate all its molecular structure, and hypothesized that the α-amino-boronic acid part of the molecule turned into 3MBut. The experimental analysis and theoretical quantum chemical calculations confirmed that the α-amino-boronic acid center of bortezomib molecule undergoes a rare and unexpected aerobic oxidation by O_2 molecule, even in catalyst and solvent-free conditions. The result of this project not only might make clear the passive source of the 3MBut peak of the OVI of bortezomib, but also, it would suggest to store this API in an inert oxygen-free atmosphere to improve the long-term and accelerated (thermal) stability of this very expensive anti-cancer drug.

Graphical abstract

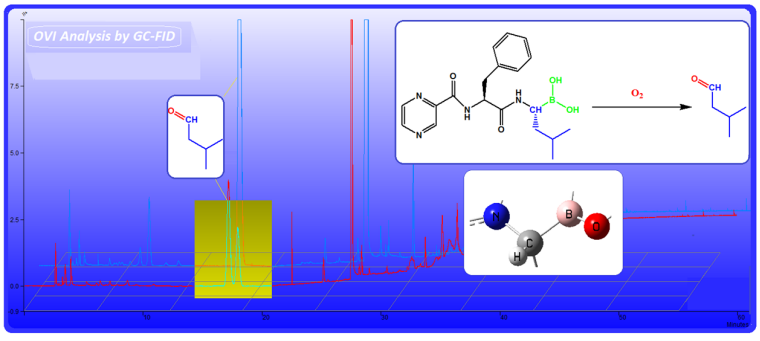

* Corresponding author.
E-mail address: M.payab@stu.umz.ac.ir (M. Payab)

doi: 10.5267/j.ccl.2021.12.001

1. Introduction

Bortezomib (BZB), as a very expensive anti-cancer API, is one of the most important chemotherapy medications which have been widely used for treatment of multiple myeloma and mantle cell lymphoma.[1] Due to the high cost of chiral precourses, difficult synthesis schemes, and low total yield, the final product of BZB (and a number of boron derivative anticancer drugs) are very expensive.[2] Many researchers such as pharmacologists, chemists, and biologists, hardly try to design[3] and synthesize[4-6] vast number of molecules which are derived from previously confirmed bioactive molecules, in order to introduce cheaper and more effective cures. It may contain theoretical drug design,[7] synthesis new derivatives, or optimizing the synthesis methods.[8,9] Also, due to the fact that, the amount of each separated impurity is important in parallel with the amount of total purity of the synthesized drugs,[10,11] finding the exact mechanism, and detecting the intermediates of the organic reactions, especially cycloadditions would help for yielding more pure products.[12-14] On the other hand, the stability of API, as well as finish product, both in long-term, and in accelerated form, is a very important issue, which could pass or reject an API for further pharmaceutical applications.[15] Thus, it is crucial that APIs especially ones like BZB as very expensive anticancers must be stable in long term storages. Or at least, suitable conditions (which would not have inverse effects on the purity, and other quality control (QC) parameters of the API), must be found. Keeping APIs in such conditions, that control the growth of each, or total impurities, and holding up the assay content of those precious matters, would lead to save hundred million dollars annually. It would subsequently lead to decrease the price of finish products. On the other hand, the OVI (which deals with the amounts of the trapped volatile solvents in the API analyzed by headspace-pressure method of GC-FID) and the *Related Impurity* (RI) analysis (which deals with the exact amounts of each separated detectable impurity as well as the total amount of impurities) are of the most important parameters in passing and releasing an API for further use. Thus, the methods which are being used for those two analyses, must be valid, and trustable.[16]

This project has been started when a problem was detected during the OVI analysis of BZB, where unknown peak (out of synthesis procedure predictions) was detected by GC-FID. Subsequently, the GC-MAS analysis showed the mentioned peak was referred to 3MBut. But what surprised us, was that in all the synthesis processes, we had not used 3MBut or any other solvent which have 3MBut as impurity (all the solvents were analyzed and no sign of 3MBut peak was detected anywhere). Thus, we concluded, there is a possibility that the passive source of 3MBut peak is the BZB itself. To examine this hypothesis, we have used both experimental (GC-FID, and GC-MAS analysis), and theoretical calculations (quantum chemical predictions and also molecular dynamic simulations). The results of both fields showed that BZB (*via* α-amino boronic acid) undergoes a rare and un-expected aerobic oxidation by molecular oxygen of air. This finding not only helped us to modify the OVI method, but also, it gave us some precious data about the thermal stability of BZB in air and improved the suitability of its packing and storage conditions.

2. Results and discussion

2.1. Experimental section

Previous reports revealed about the destruction of boronic acids in solvents like water leading to oxidation of boron to give a hydrogenated alkyl (R-H), and boric acid (scheme 1-a).[17] While the GC-MAS, and GC-FID chromatogram data showed us that this mechanism could not be true in the case of BZB; because, the carbon center of this (α-amino) boronic acid undergoes an oxidation process to give an aldehyde (3MBut; m/z: 29,44,58,71,86; similarity index based on *Wiley Library*=95%). Also, some of the last recent reports revealed about the successful intervention of molecular oxygen in aerobic oxidation of some boronic acids in presence of metal catalysts like 20% molar of Cu in acetonitrile (as solvent), alcohol, and pyridine (as base) leading to production of ketones (Scheme 1-b).[18]

Unlike usual boronic acids, BZB could be reacted with molecular oxygen even in a solvent-free condition. However, this process is amplified in solvents like water, or hydrogen peroxide (H_2O_2) in water. The main difference between the boronic acid of BZB and other usual boronic acid, is the amino group which is placed in the alpha position carbon. We had estimated that this amino group may intervene in aerobic oxidation of boron and the alpha carbon.
For a better understanding of this issue, we used another compound containing α-amino boronic acid. In this examination, 0.03 gr of Boroleu was placed in the same condition (40 min, 80ºC) in 5ml of deionized water, acetonitrile, (1ml H_2O_2 3% and 5ml deionized water), aerobic, and inert system (Figure 1; Scheme 1-d). The results showed that Boroleu is oxidized in water, hydrogen peroxide, and solvent-free (aerobic atmosphere) like BZB to give 3MBut as the same aldehyde even in solvent-free condition (Scheme 1-c). Also, in degassed acetonitrile, and in inert system, any peak related to 3MBut was not observed (like BZB).

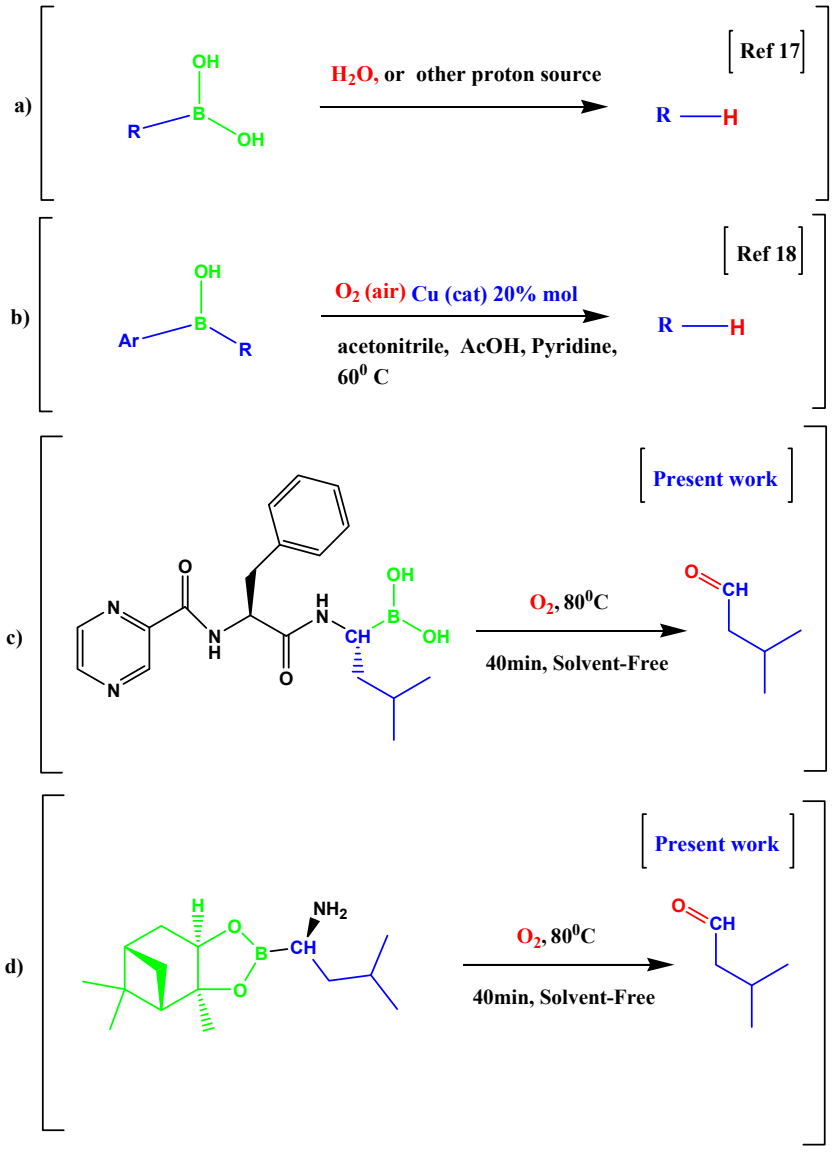

Scheme 1. Oxidation of BZB by molecular oxygen, compared to usual boronic acids

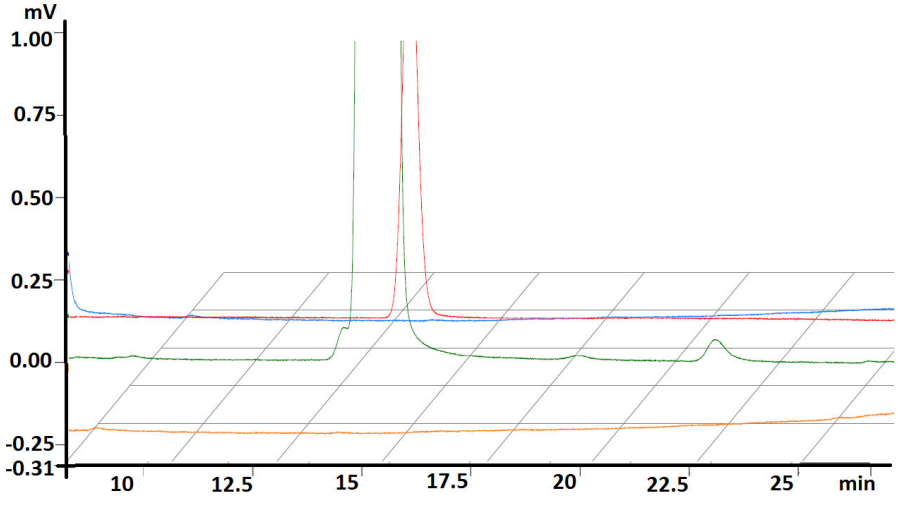

Fig. 1. the effect of environment changes on the growth of 3MBut peak area, in constant temperature (blue, red, green, and yellow lines for acetonitrile, H_2O, H_2O_2, and inert surrounding, respectively).

In these experiments (previous reports about simple boronic acids, and present results from BZB, and Boroleu, aerobic oxidation), what was in common, was the existence of an amino functional group on the α-position carbon of boronic acid (or boronic ester). Also, production of 3MBut by α-boronic acid (or ester) as precursors, in presence of molecular oxygen in one hand, and stopping the production of this aldehyde in inert atmosphere or in degassed acetonitrile, led us to the idea that the α-boronic acid (or ester) undergoes an unexpected aerobic oxidation by O_2 molecule. Table 2 shows the results of the GC-FID experiment.

Table 2. the effect of solvent changes on the growth of 3MBut (m/z: 29,44,58,71,86; Similarity index by *Wiley Library*=95%) peak area

	Sample Weight (mgr)	Temperature (°C)	Solvent(s) (ml)	Peak area of 3MBut ($mV.S^{-1}$)
Boroleu	50	80	(inert system)	-
Boroleu	50	80	Acetonitrile (5 ml)	-
Boroleu	50	80	Water (5 ml)	13753
Boroleu	50	80	Water (5ml) +H_2O_2 3% (1ml)	2757105
BZB	50	80	(inert system)	-
BZB	50	80	Acetonitrile (5 ml)	-
BZB	50	80	Water (5 ml)	49822

As shown in **Table 2**, both Boroleu, and BZB would not be oxidized (do not produce 3MBut) in an inert atmosphere or degassed and oxygen free solvents like acetonitrile. While both of them could release that aldehyde in atmosphere or in solvent like water (13753$mV.S^{-1}$, and 49822$mV.S^{-1}$, for Boroleu, and BZB, respectively). Also, H_2O_2 which produces molecular oxygen in water, significantly increases the 3MBut in headspace pressure up to 2757105 $mV.S^{-1}$(about 200 times more than the same condition in pure water). These results would experimentally confirm the possibility of oxidation of BZB, and Boroleu (which contain α-amino boronic acid) by the molecular oxygen of air.

Table 3. the effect of temperature changes on the growth of 3MBut peak area, in atmospheric systems. mg represents the milligram unit

	Sample Weight (mg)	Temperature (°C)	System	Peak area of 3MBut ($mV.S^{-1}$)
Boroleu	50	60	Atmosphere	561
BZB	50	80	Atmosphere	13476
Boroleu	50	80	Atmosphere	4351
Boroleu	50	100	Atmosphere	12927
Boroleu	50	120	Atmosphere	60938

On the other hand, the results of **Table 3** (**Fig. 2**) showed that increasing the temperature (60ºC, 80ºC, 100ºC, and 120ºC) significantly increase the rate of this oxidation reaction; somehow, the peak area related to 3MBut grows from 561, 4351, 12927, and 60938$mV.S^{-1}$, for atmospheric oxidation of Boroleu at 60, 80,100, and 120ºC, respectively.

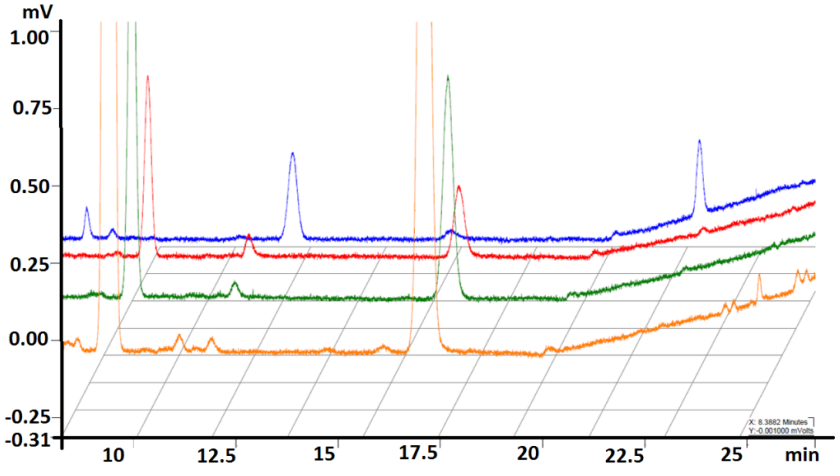

Fig. 2. the effect of temperature changes on the growth of 3MBut peak area, in atmospheric systems (blue, red, green, and yellow lines for 60ºC, 80ºC, 100ºC, and 120ºC, respectively)

2.2. *Theoretical section*

To answer the question "what causes the α-amino boronic acid (or ester) to react with molecular oxygen and produce aldehyde, instead of R-H (like usual boronic acids)?" We aided the theoretical quantum chemical calculations. To do this, at the first step, we chose the active center of α-amino boronic acid and reacted with both usual boronic acid, and α-amino substitute of that, with molecular oxygen. In order to reach more trustable data for the probable structures which may emerge during the chemical absorption process of the molecular oxygen of air, by boronic acid (BA), and α-amino boronic acid (ABA), we have used the *Born-Oppenheimer* molecular dynamics (BOMD) simulation (see **Fig. 3**), in parallel with mental prediction for designing the input structures. Then, all candidate stable and meta-stable structures have been taken under quantum chemical calculations preceded by *Gaussian* 2003 quantum chemical packages which was mentioned above.

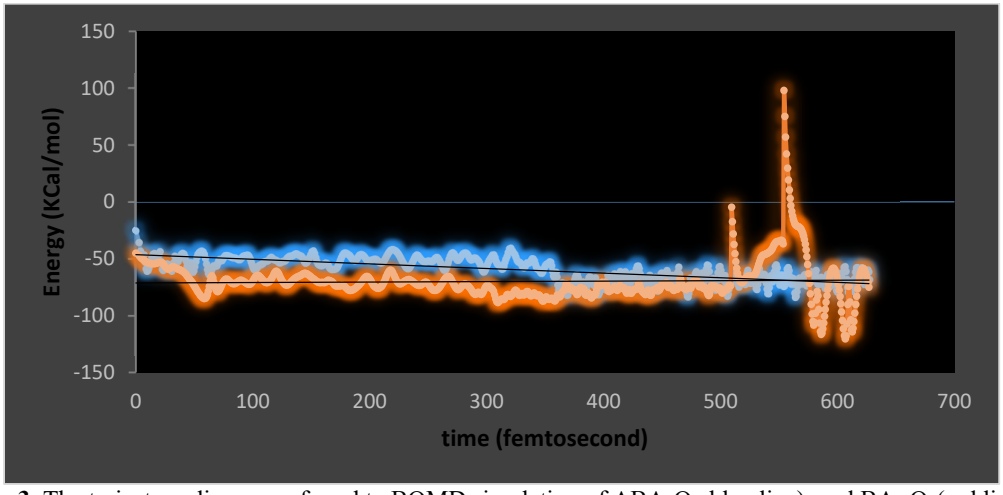

Fig. 3. The trajectory diagram referred to BOMD simulation of ABA-O_2 (blue line), and BA- O_2(red line).

Also, several hypothetical structures with different orientations were designed and drawn by gauss view software and putted under quantum chemical calculation, to find any probable species which may emerge during the first step of primary adsorption or even the first step of chemical reaction between the molecular oxygen and the reactants (**Fig. 4**). Then, a diagram containing the reaction pathways of adsorption (or reaction) of molecular oxygen and the BA, and ABA, based on the potential energy surface (PES), was designed (**Fig. 5**).

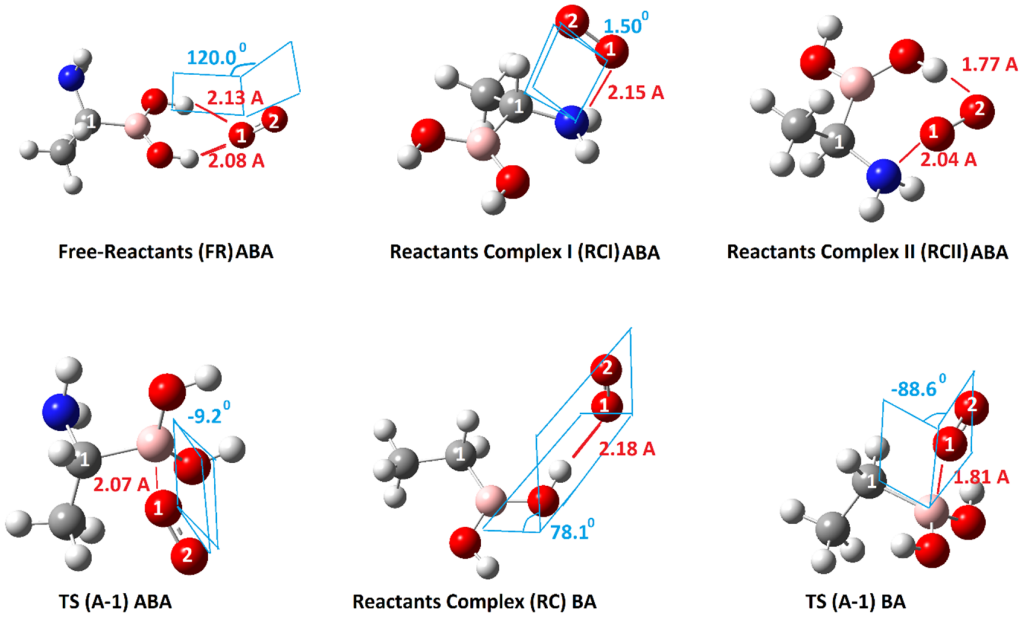

Fig. 4. The chemical structures which could emerge during the aerobic oxidation of BA, and ABA, by molecular oxygen, calculated at B3LYP/6-311++G(d,p) level of theory

The results of the calculations showed that in the case of ABA, at least two reactants complex (RC)s, and a free-reactant (FR) with different orientations could exist before the absorption proceeds. Somehow, at the first step, the O1 atom of O_2 molecule closes to ABA and is stabilized by hydrogens of boronic acids in about 2.1 Å (see FR-ABA in **Fig. 1**) 0.0 kcal.mol^{-1}. Then, it closes to the C1 of ABA more and more (as well as losing energy) to form RCI-ABA (-9.2 kcal.mol^{-1}), and RCII-ABA (-10.2 kcal.mol^{-1}), respectively. In the RCII-ABA system, O1 of O_2 molecule receives energy (+15.8 kcal.mol^{-1}) and attacks to the boron atom of ABA to form TS (A-1)-ABA (+5.6 kcal.mol^{-1}; the negative imaginary freq= -192.32 cm^{-1}). On the other hand, if the FR-ABA species path through a direct energy tunnel (instead of other meta-stable energy stations like RCI, or RCII) to reach the energy peak of TS (A-1)-ABA (a B···O1 distance of 2.07 Å), the total energy barrier for adsorption of chemical absorption of O_2 decreases to only +5.6 kcal.mol^{-1}. Also, in the case of the absorption of O_2 by BA, the RC-BA (a dihedral angle of 78.1°; an O1···H distance of 2.18 Å) receives energy and transforms into the energy peak of TS (A-1)-BA with an energy barrier of +15.2 kcal.mol^{-1} (the negative imaginary freq= -334.09 cm^{-1}), (**Fig. 5**).

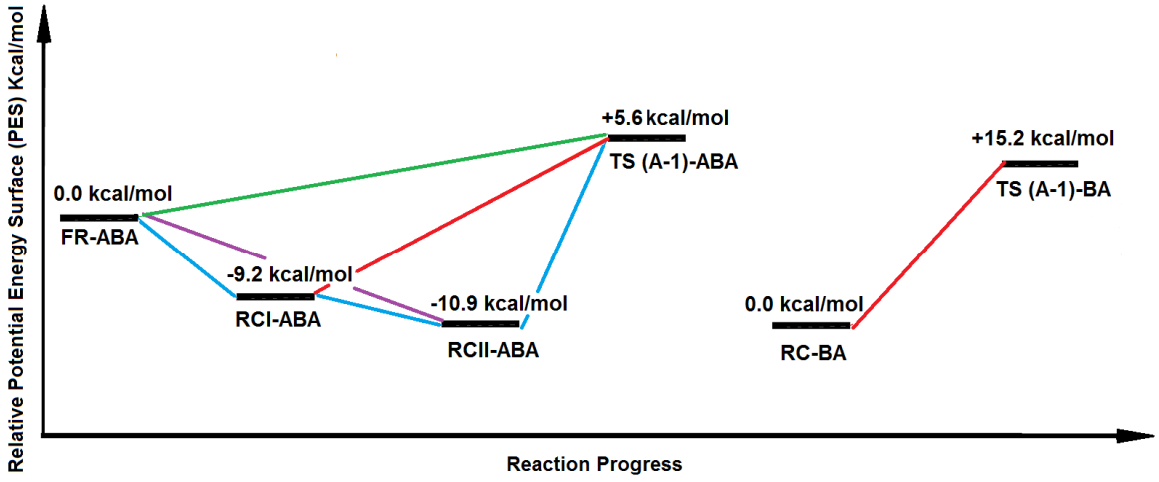

Fig. 5. The reaction pathways of adsorption of O_2 by BA, and ABA, based on the potential energy surface, calculated at B3LYP/6-311++G(d,p) level of theory.

Thus, the main potential energy barrier for absorption of the molecular oxygen by ABA is about +5.6 kcal.mol^{-1} which shows a very fast and favorable reaction compared to absorption of O_2 by a usual boronic acid (15.2 kcal.mol^{-1}). This could be the key reason for the unexpected oxidation reaction of BZB compound by molecular oxygen of the air which makes it unstable in long-term stability analysis as well as emergence of 3MBut peak in OVI analysis.

3. Conclusions

The most important result of this work is; the carbon center of the α-amino boronic acid (ester) of bortezomib undergoes an unpleasant aerobic oxidation by O_2 molecule, leading to thermal decomposition of this very expensive anti-cancer drug. The experimental data showed that the Boroleu, and BZB could not be oxidized (do not produce 3MBut) in an inert atmosphere or degassed and oxygen free solvents like ACN. While both those compounds could release that aldehyde in solvent-free atmospheric system as well as in solvents like water (13753 mV.S^{-1}, and 49822 mV.S^{-1}, for Boroleu, and BZB, respectively; all sampling procedures were head-space vapor collection). Also, H_2O_2 which produces molecular oxygen in water, significantly increases the 3MBut in headspace pressure up to 2757105 mV.S^{-1} (about 200 times more than the same condition in pure water). These results would experimentally confirm the possibility of oxidation of BZB, and Boroleu (which contain α-amino boronic acid) by the molecular oxygen (of air).

On the other hand, the theoretical results indicate that the potential energy barrier for absorption reaction of the molecular oxygen by ABA is about +5.6 kcal.mol^{-1} which is significantly favorable compared to the absorption process of O_2 by a usual boronic acid (15.2 kcal.mol^{-1}). This could be the key reason for the unexpected oxidation reaction of BZB compound by molecular oxygen of the air which makes it unstable in long-term stability analysis as well as emergence of 3MBut peak in OVI analysis. We suggest that in the future research, both the accelerated and long-term stability of this precious anticancer will be examined under an inert atmosphere.

Acknowledgment

Authors would like to thank Tofigh Daru Research and Engineering Company for financial and technical support of this work.

4. Materials and methods

4.1. Experimental section

4.1.1. Reagents

Chemicals containing, (R)-BoroLeu-(+)-Pinanedioltrifluoroacetate (Boroleu), acetonitrile, H_2O_2, methanol were prepared from Merck chemical company (Germany). Also, the BZB API was provided from the *Chemical Synthesis Department of Tofigh Daru Research and Engineering Company* (Tehran, Iran).

4.1.2. Instrumentation

The OVI analyses were performed using a GC-FID system (CP-3800, GC Varian, equipped with CTC Combi-Pal headspace autosampler injection containing an incubator. A capillary column (the Agilent J&W CP-Select 624 CB, length 30m, internal diameter 0.53 mm, and film thickness 3.0 µm GC column, with an optimized G43 stationary phase) was used for separation of the gaseous specious. The carrier gas was nitrogen, and the flow rate of the system was about 6 ml min^{-1}. The GC-MS analysis was performed using a GC-MS system (GCMS-QP 2010 SE: mass selective **detector** MSD, operated in the EI mode (electron energy = 70 eV), scan range = 45-400 amu, and scan rate = 3.99 scans/sec (Shimadzu Corporation). A capillary column (the Agilent J&W CP-Sil8 CB, length 50m, internal diameter 0.53 mm, and film thickness 1.0 µm GC column) was used for separation of the gaseous specious. The carrier gas was helium, and the flow rate of the system was about 2 ml min^{-1}.

A 0.05 g amount of BZB, (or Boroleu) samples were dissolved in 5ml of water and were incubated for about 40 min. then, 1000 µl of headspace vapor of the vial was injected to the column. After separation in the GC-column with a special temperature programming with some modifications compared to the other methods,[19] the sample was ionized and detected applying the helium plasma in the BID at 270°C. The detailed operating method of the analysis was described in Table 1.

Table 1. The gas chromatography conditions set for analyzing the OVI contents of the synthesized BZB

order	Parameter	Value
(A) Injector setting		
1	Injector temp.	155º C
2	Carrier gas	Nitrogen
3	Split ratio	2
(B) Oven setting		
4	Initial oven temp.	50º C
5	Hold time	18 min
6	secondary oven temp.	250 º C
7	secondary Hold time	15 min
8	Rate	10 º C/min
9	Column flow	6 ml/min
10	Purge flow	2 ml/min
(C) column		
11	Column type	G-43
12	Column length	60 m
13	Inner Diameter	0.53 mm
14	Film thickness	3 µm
(D) Detector		
15	Detector temp.	270º C
16	Discharge gas	-

4.2. Theoretical section

Several hypothetical structures with different orientations were developed as input files for each predicted energy state and optimized to give any possible stable or meta-stable system. As a result, a number of stable and metastable energy stations were found for the reactants, and the transition states (TS)s. The Gaussian 03 chemical quantum package[20] was used to perform all of the calculations, and the density functional theory (DFT) procedure in B3LYP/6-311++G(d,p) theoretical level was applied for optimizing the possible structures.[21,22] The TS structures were found by using the synchronous transit-guided quasi-Newton (STQN) approach,[23,24] and the frequencies of each optimized structure were extracted for calculating the thermodynamic energies for each possible state. All the simulations were performed by using the BOMD method which is widely used for the same calculations.[25]

References

1 Zhang S., Kulkarni A. A., Xu B., Chu H., Kourelis T., Go R. S., Wang Y. (**2020**) Bortezomib-based consolidation or maintenance therapy for multiple myeloma: a meta-analysis, *Blood cancer J.*, 10 1-9.

2 Yates S., Matevosyan K., Rutherford C., Shen Y. M., Sarode R. (**2014**) Bortezomib for chronic relapsing thrombotic thrombocytopenic purpura: a case report, *Transfusion* 54 2064-2067.

3 Houssein E. H., Hosney M. E., Elhoseny M., Oliva D., Mohamed W. M., Hassaballah M. (**2020**) Hybrid Harris hawks optimization with cuckoo search for drug design and discovery in chemoinformatics, *Sci. Rep.* 10 1-22.

4 Panda P., Chakroborty S. (**2020**) Navigating the Synthesis of Quinoline Hybrid Molecules as Promising Anticancer Agents, *Chem. Select* 5 10187-10199.

5 a) Bakherad M., Keivanloo A., Samangooei S., Omidian M. (**2013**) A phenyldithiocarbazate-functionalized polyvinyl chloride resin-supported Pd (II) complex as an effective catalyst for solvent-and copper-free Sonogashira reactions under aerobic conditions, *J. Organomet. Chem.* 740 78-82; b) Bakherad M., Keivanloo A., Siavashi M., Omidian M. (**2014**) Three-component synthesis of imidazo [1, 2-c] pyrimidines using silica sulfuric acid (SSA). *Chinese Chem. Lett.* 25 149-151.

6 a) Rostami-Charati F., Hossaini Z., Sheikholeslami-Farahani F., Azizi S., Siadati S. A. (**2015**) Synthesis of 9H-furo [2, 3-f] Chromene Derivatives by Promoting ZnO Nanoparticles. *Comb. chem. high throughput screen.* 18 872-880; b) Hossaini Z., Rostami-Charati F., Ghambarian M., Siadati S. A. (**2015**) Synthesis of a new class of phosphonate derivatives using a three component reaction of trialkylphosphites or triarylphosphites in water. *Phosphorus Sulfur Silicon Relat. Elem.* 190 1177-1182; c) Dadras A., Rezvanfar M. A., Beheshti A., Naeimi S. S., Siadati S. A. (**2021**) An Urgent Industrial Scheme both for Total Synthesis, and for Pharmaceutical Analytical Analysis of Umifenovir as an Anti-Viral API for Treatment of COVID-19, *Comb. Chem. High Throughput Screen*. 24. Accepted manuscript, DOI: 10.2174/1386207324666210203175631.

7 Sydow D., Morger A., Driller M., Volkamer A. (**2019**) TeachOpenCADD: a teaching platform for computer-aided drug design using open source packages and data. *J. cheminformatics* 11 1-7.

8 a) Grzelak P., Utecht G., Jasiński M., Mlostoń G. (**2017**) First (3+ 2)-cycloadditions of thiochalcones as C= S dipolarophiles: efficient synthesis of 1, 3, 4-thiadiazoles via reactions with fluorinated nitrile imines. *Synthesis* 49 2129-2137; b) Bakherad M., Keivanloo A., Omidian M., Samangooei S. (**2014**) Synthesis of pyrrolo [2, 3-b] pyrazines through Sonogashira coupling reaction of 5, 6-dichloropyrazine-2, 3-dicarbonitrile with hydrazine, phenylacetylene and various aldehydes. *J. Chem. Res*. 38 762-764.

9 Jasiński R., Żmigrodzka M., Dresler E., Kula K. (**2017**) A Full Regioselective and Stereoselective Synthesis of 4-Nitroisoxazolidines via Stepwise [3+ 2] Cycloaddition Reactions between (Z)-C-(9-Anthryl)-N-arylnitrones and (E)-3, 3, 3-Trichloro-1-nitroprop-1-ene: Comprehensive Experimental and Theoretical Study. *J. Hetero. Chem*. 54 3314-3320.

10 Sova M., Frlan R., Gobec S., Časar Z. (**2020**) Efficient and Straightforward Syntheses of Two United States Pharmacopeia Sitagliptin Impurities: 3-Desamino-2, 3-dehydrositagliptin and 3-Desamino-3, 4-dehydrositagliptin. *ACS omega* 5 5356-5364.

11 Guo K., Zhang T., Wang Y., Jin B., Ma C. (**2019**) Characterization of degradation products and process-related impurity of sutezolid by liquid chromatography/electrospray ionization tandem mass spectrometry. *J. pharma. Biomed. Anal.* 169 196-207..

12 a) Jasiński R., Dresler E. (**2020**) On the question of zwitterionic intermediates in the [3+ 2] cycloaddition reactions: A critical review. *Organics*, 1 49-69; b) Jasiński R., Mikulska M., Barański A. (**2013**) An experimental and theoretical study of the polar [2+ 3] cycloaddition reactions between 1-chloro-1-nitroethene and (Z)-C-aryl-N-phenylnitrones. *Cent. Europ. J. Chem.* 11 1471-1480; c) Siadati S. A. (**2015**) An example of a stepwise mechanism for the catalyst-free 1, 3-dipolar cycloaddition between a nitrile oxide and an electron rich alkene. *Tetrahedron let*. 56 4857-4863; d) Siadati S. A. (**2016**) Beyond the alternatives that switch the mechanism of the 1, 3-dipolar cycloadditions from concerted to stepwise or vice versa: a literature review. *Prog. Reac. Kinet. Mech*. 41 331-344.

13 a) Chen M., He C. Q., Houk K. N. (**2019**) Mechanism and Regioselectivity of an Unsymmetrical Hexadehydro-Diels–Alder (HDDA) Reaction. *J. Org. Chem.* 84 1959-1963; b) Siadati S. A. (**2016**) The Effect of Position Replacement of Functional Groups on the Stepwise character of 1, 3-Dipolar Reaction of a Nitrile Oxide and an Alkene. *Helve. Chim. Acta* 99 273-280; c) Siadati S. A. (**2016**) A Theoretical Study on Stepwise-and Concertedness of the Mechanism of 1, 3-Dipolar Cycloaddition Reaction Between Tetra Amino Ethylene and Trifluoro Methyl Azide. *Comb. Chem. high throughput screen*. 19 170-175.

14 a) Firestone R. A. (**2013**) The Low Energy of Concert in Many Symmetry-Allowed Cycloadditions Supports a Stepwise-Diradical Mechanism. Intern. *J. Chem. Kinet.* 45 415-428; b) Mohtat B., Siadati S. A., Khalilzadeh M. A., Zareyee D. (**2017**) The concern of emergence of multi-station reaction pathways that might make stepwise the mechanism of the 1, 3-dipolar cycloadditions of azides and alkynes. *J. Mol. Struct.* 1155, 58-64.

15 Kasabe A., Yadav A., Veer V. (**2020**) Consideration of stability study in pharmaceutical product: A Review. *J. Current Pharma Res.* 10 3832-3847.

16 Naz A., Sher N., Siddiqui F. A., Kashif M., Ansari A. (**2019**) Simultaneous analysis of daclatasvir with its three organic impurities: Application in stability studies, pharmaceuticals and serum samples. *Microchem. J.* 147 797-805.

17 Cox P.A., Reid M., Leach A. G., Campbell A. D., King E. J., Lloyd-Jones G. C. (**2017**) Base-Catalyzed Aryl-B(OH)2 Protodeboronation Revisited: From Concerted Proton Transfer to Liberation of a Transient Aryl Anion, *J. Am. Chem. Soc*. 139 13156-13165.

18 Grayson J. D., Partridge B. M. (**2019**) Mild cu-catalyzed oxidation of Benzylic Boronic esters to ketones, *ACS Catal.* 9 4296-4301.

19 USP, Crospovidone (**2016**) "USP 39-NF 34." Rockville, MD, USA, 838.

20 Frisch M. J., Trucks G. W., Schlegel H. B., Scuseria, G. E. et al. (**2003**) GAUSSIAN 03, Gaussian Inc. Pittsburgh, PA.
21 Becke A. D. (**1988**) Density-functional exchange-energy approximation with correct asymptotic behavior, *Phys. Rev. A* 38 3098-3100.
22 a) Delchev V., Nenkova M. V. (**2008**) Theoretical Modeling of the Ground State Intermolecular Proton Transfer in Cytosine: DFT Level Study, *Acta. Chim. Slov.* 55 132-137; b) Kącka-Zych A., Radomir J. (**2020**) Molecular mechanism of Hetero Diels-Alder reactions between (E)-1, 1, 1-trifluoro-3-nitrobut-2-enes and enamine systems in the light of Molecular Electron Density Theory, *J Mol. Graph. Model*. 101 107714; c) Kula K., Kącka-Zych A., Łapczuk-Krygier A., Wzorek Z., Nowak A. K., Jasiński R. (**2021**) Experimental and Theoretical Mechanistic Study on the Thermal Decomposition of 3, 3-diphenyl-4-(trichloromethyl)-5-nitropyrazoline. *Molecules* 26 1364; d) Jasiński R., Agnieszka Kącka A. (**2015**) A polar nature of benzoic acids extrusion from nitroalkyl benzoates: DFT mechanistic study, *J. Mol. Model*. 21 1-7.
23 Peng C., Ayala P. Y., Schlegel H. B., Frisch M. J. (**1996**) Using redundant internal coordinates to optimize equilibrium geometries and transition states, *J. Comput. Chem*. 17 49-56.
24 Peng C., Schlegel H. B. (**1993**) Combining synchronous transit and quasi-newton methods to find transition states, *Isr. J. Chem*. 33 449-454.
25 Pu M., Privalov T. (**2015**) Ab initio molecular dynamics with explicit solvent reveals a two-step pathway in the frustrated Lewis pair reaction, *Chem.–A Europ. J.* 21 17708-17720.